Genome-Scale reconstruction of *Paenarthrobacter aurescens* TC1 metabolic model towards the study of atrazine bioremediation

Shany Ofaim[1,2* ɨ], Raphy Zarecki[1*], Seema Porob[3], Daniella Gat[3], Tamar Lahav[1], Xihui Xu[1, 4], Yechezkel Kashi[2], Radi Aly[1], Jiandong Jiang[4], Hanan Eizenberg[1], Zeev Ronen[3 ϯ] & Shiri Freilich[ɨ1ϯ]

[1]Newe Ya'ar Research Center, Agricultural Research Organization, Ramat Yishay, Israel, [2]Faculty of Biotechnology and Food Engineering, Technion-Israel Institute of Technology, Haifa, Israel, [3]Department of Environmental Hydrology & Microbiology, Zuckerberg Institute for Water Research, Jacob Blaustein Institutes for Desert Research, Ben-Gurion University of the Negev, Midreshet Ben-Gurion, 8499000, Israel, [4]Department of Microbiology, Agricultural University of Nanjing, No. 6 Tongwei RD, 210095, Nanjing, Jiangsu Province, China

*equal contribution

ϯ equal contribution

ɨ Corresponding author

email address (in the order of author list): shashany@gmail.com, raphy.zarecki@gmail.com, porob@post.bgu.ac.il, gat.daniella@gmail.com, lahav008@gmail.com, xuxihui01@gmail.com, kashi@technion.ac.il, radi@volcani.agri.gov.il, jiang_jjd@njau.edu.cn, eizenber@volcani.agri.gov.il, zeevrone@bgu.ac.il, shiri.freilich@gmail.com.

ABSTRACT

Atrazine is an herbicide and pollutant of great environmental concern that is naturally biodegraded by microbial communities. The efficiency of biodegradation can be improved through the stimulating addition of fertilizers, electron acceptors, etc. In recent years, metabolic modelling approaches have become widely used as an *in silico* tool for organism-level phenotyping and the subsequent development of metabolic engineering strategies including biodegradation improvement. Here, we constructed a genome scale metabolic model, *i*RZ960, for *Paenarthrobacter aurescens* TC1 – a widely studied atrazine degrader - aiming at simulating its degradation activity. A mathematical stoichiometric metabolic model was constructed based on a published genome sequence of *P. aurescens* TC1. An Initial draft model was automatically constructed using the RAST and KBase servers. The draft was developed into a predictive model through semi-automatic gap-filling procedures including manual curation. In addition to growth predictions under different conditions, model simulations were used to identify optimized media for enhancing the natural degradation of atrazine without a need in strain design via genetic modifications. Model predictions for growth and atrazine degradation efficiency were tested in myriad of media supplemented with different combinations of carbon and nitrogen sources that were verified *in vitro*. Experimental validations support the reliability of the model's predictions for both bacterial growth (biomass accumulation) and atrazine degradation. Predictive tools, such as the presented model, can be applied

for achieving optimal biodegradation efficiencies and for the development of ecologically friendly solutions for pollutant degradation in changing environments.

KEYWORDS

Genome scale metabolic models; Flux Balance Analysis; *Paenarthrobacter aurescens* TC1; atrazine; bioremediation

Background

Areas contaminated with hazardous materials are rapidly increasing worldwide introducing a need in remediation approaches. Bioremediation - an environmental bioprocess in which naturally occurring organisms are used for breaking down hazardous substances into less toxic or non-toxic substances, is increasingly acknowledged as a cost-effective strategy for environmental cleaning (Kanissery and Sims 2011; Kastner and Miltner 2016). As critical environmental bioprocesses carried by bacteria are either related to removal of pollutants from water, soil or air or involved in the production of commercially valuable compounds (Perez-Garcia et al. 2016), bacterial bioremediation is widely applied for the degradation of various organic pollutants (Mani and Kumar 2013; Megharaj et al. 2011; Nilsson et al. 2013; Shah and Dahanukar 2012) such as herbicides (Fan and Song 2014; Megharaj et al. 2011; Nousiainen et al. 2015; Sagarkar et al. 2014; Singh and Singh 2016). Bioremediation may occur naturally or through the stimulating addition of fertilizers, electron acceptors, etc. These amendments encourage the growth of the degrading microbes within the medium or environment in a process termed biostimulation (Adams et al. 2015; Kanissery and Sims 2011).

72 Atrazine is an herbicide and pollutant of great environmental concern. Its residues are
73 still found in soil samples decades after it was last applied. These residues were shown
74 to chronically leach into the local aquifer (Abubucker et al. 2012). Atrazine has been
75 widely reported to be biodegraded by bacteria (Chen et al. 2014; Fan and Song 2014;
76 Monard et al. 2011; Nousiainen et al. 2015; Sagarkar et al. 2013; Sagarkar et al. 2014;
77 Udikovic-Kolic et al. 2012; Wang and Xie 2012; Xie et al. 2013; Zhang et al. 2012). One
78 of the well-known atrazine degraders is *Paenarthrobacter aurescens* TC1 (Fang et al.
79 2015; Sagarkar et al. 2013; Strong et al. 2002; Wang and Xie 2012; Zhang et al. 2012).
80 *P. aurescense* TC1 is described as nutritionally versatile bacterium that is capable of
81 utilizing a wide array of complex metabolites, including agriculturally used herbicides
82 (Deutch et al. 2018; Mongodin et al. 2006). The full hydrolytic pathway for atrazine
83 degradation was reported and described in *P. aurescens* TC1. Intermediates, created
84 in the degradation process are further metabolized by the organism and can provide
85 sole sources for carbon and nitrogen (Strong et al. 2002). This bacterium was
86 previously reported to biodegrade atrazine much more efficiently than most atrazine
87 degrading bacteria including *Pseudomonas* sp. ADP (Silva et al. 2015). While PADP can
88 only use the hydrolytic products of the ring cleavage as nitrogen but not as carbon;
89 TC1 can use the side groups of atrazine as source for carbon, nitrogen and energy
90 consuming up to 3,000 mg of atrazine per liter (Strong et al. 2002). As such, *P.*
91 *aurescens* TC1 can be a model for the study of atrazine bioremediation.
92 Modern tools of genomics, transcriptomics, metabolomics, proteomics, signaling
93 systems and synthetic biology have opened new avenues for biotechnological
94 advances and are increasingly applied for promoting better understanding of complex
95 biological systems. In recent years, constraint based metabolic modelling approaches

96 have become widely used as an *in silico* tool for organism-level phenotyping and the
97 subsequent development of metabolic engineering strategies (Contador et al. 2015;
98 Xu et al. 2013). Generally, such approaches follow four key steps: (1) data acquisition
99 – mainly genome sequencing information, basic cell-physiological and biochemical
100 knowledge and some experimental data on cell growth; (2) model reconstruction -
101 translating data into structured mathematical representation; (3) constraint-based
102 optimization simulations - the prediction of growth rate, substrate uptake rates, and
103 byproduct rates under different growth conditions or following knockout mutations,
104 in the absence of kinetic information (Lee et al. 2008; Mahadevan et al. 2006;
105 Mahadevan and Lovley 2008; Oberhardt et al. 2015; Price et al. 2003; Reed et al. 2003;
106 Thiele et al. 2005); and (4) experimental validation. The potential of such models for
107 the investigation of optimal processing is now acknowledged and practiced (Biswas et
108 al. 2015; Fang et al. 2011; Henson 2015; Perez-Garcia et al. 2016; Zomorrodi and Segre
109 2016). Examples for applicative use include the optimal production or utilization of
110 industrial compounds such as xylose (Cordova et al. 2015), biofuels (de la Torre et al.
111 2015) and vitamins (Zou et al. 2012). In bioremediation, genome scale metabolic
112 modeling approaches were applied for the design of *Geobacter sulfurreducens* strain
113 capable of increased electron transfer and a higher Fe(III) respiratory that was
114 beneficial for environmental bioremediation (Izallalen et al. 2008). Strain design is
115 often based on the Optknock algorithm (Burgard et al. 2003) and its derivatives which
116 search for the optimal gene knockouts for a desired metabolic production. However,
117 unlike industrial use of engineered strain for enhanced production in monoculture,
118 introduction of exogenous species into natural habitat is far from trivial and hampers
119 the application of modeling approaches towards bioremediation solutions. An

120 alternative strategy is the use of modeling for the design of optimal conditions that
121 will enhance processes (degradation or synthesis) carried by the endogenous
122 community. In a recent project we demonstrate the use of metabolic models for
123 predicting interactions between *P.aurescens* TC1 and endogenous soil species.
124 Exchange metabolites secreted by non-degraders species contribute for enhancing
125 *P.aurescens* TC1 growth and expediting degradation efficiency (Xu et al. 2019). Here,
126 we describe in detail the process of manual curation of *P.aurescens* TC1 draft
127 metabolic model, its application for predicting growth and atrazine degradation in
128 media containing different carbon and nitrogen sources based on a dynamic (capable
129 of reporting changes over time) and non-dynamic flux based algorithms, and the
130 experimental testing of the predictions.

131

132 **Materials and Methods**

133 Reconstruction of the initial draft for *P. aurescens* TC1 metabolic model

134 An initial draft model of *P. aurescens* TC1 was reconstructed as described in (Xu et al.
135 2019). Briefly, the genome sequence of *P. aurescens* TC1 was retrieved from NCBI
136 (GenBank accession id. NC_008711), uploaded into RAST (Meyer et al. 2008), spliced
137 into genes and annotated. RAST annotations were put through the Model SEED
138 pipeline (Henry et al. 2010) and an initial metabolic network reconstruction was
139 obtained. This initial reconstruction contained a list of reactions classified as exchange,
140 transport, and cytosolic as well as a list of all relevant metabolites and a biomass
141 reaction. The composition of the biomass reaction summarizes the fractional
142 contribution of a generalized microbial biomass precursors (e.g., amino acids and

143 lipids) to the synthesis of a new cell, as provided in the draft reconstructions from
144 Model SEED and KBase. Unspecified non-metabolic consuming processes in the cell
145 were defined as ATP maintenance and set similarly to (Oh et al. 2007). Missing
146 reactions were filled through an automatic gap-filling procedure, using default
147 (optimal) media options (Henry et al. 2010). The model was exported from KBase in
148 SBML format (Additional File 4).
149
150 Model curation and evaluation
151 Manual curation procedures were carried to adapt model performances to reported
152 physiological capacities. Simulation conditions were modified to reflect
153 experimentally validated minimal media alternatives that support growth of *P.*
154 aurescnes TC1 (Strong et al. 2002). Missing reactions (network gaps) were filled based
155 on integrating information extracted from public databases such as KEGG (Kanehisa
156 and Goto 2000; Kanehisa et al. 2014), Uniprot (UniProt 2015), and JGI databased
157 (Kanehisa et al. 2012; Nordberg et al. 2014; UniProt 2015) (Additional File 1). The
158 procedures required the following steps: (1) Identifier standardization - reaction
159 identifiers from the different databases were converted into KBASE rxn accessions and
160 added to the model; (2) Reaction reversibility calibration according to the KEGG
161 scheme; (3) Reaction elemental and redox balance verification; and (4) removal of
162 futile loops – active internal (non-exchange) reactions which remained active while all
163 external fluxes were blocked (upper and lower bounds set to zero). Remaining gaps
164 were then manually filled by an extensive literature survey and the use of other public
165 resources (Additional File 2).

166 All curation procedures were carried iteratively versus growth simulations to ensure
167 the production of all biomass components in Minimal Mineral Media (MMM: K^+, Mn^{2+},
168 CO2, Zn^{2+}, SO_4^-, Cu^{2+}, Ca^{2+}, HPO_4^{2-}, Mg^{2+}, Fe^{2+}, Cl^-), supplemented by alternative carbon
169 and nitrogen sources including atrazine, ethylamine, isopropylamine, ammonia,
170 glucose and selected amino acids (Additional File 3). As part of the curation process,
171 the hydrolytic pathway of atrazine degradation was *a priori* added to the model based
172 on previously published experimental data (Strong et al. 2002).
173
174 Flux balance analyses simulations and dynamic, time dependent simulations
175 Flux distributions in the metabolic model were determined using Flux Balance Analysis
176 (FBA) (Orth et al. 2010; Thiele and Palsson 2010; Varma and Palsson 1994). Briefly, a
177 metabolic model includes a network that is described as a stoichiometric matrix $\mathbf{S}_{m \times n}$,
178 where *m* represents the number of metabolites and *n* the number of reactions in the
179 model. In the assumed pseudo-steady-state, internal metabolites concentrations and
180 fluxes are assumed to be constant. The model can be represented as: $\mathbf{S} \times v = 0$, where
181 vector v signifies the fluxes through the internal reactions. As the number of reactions
182 (*n*) typically exceeds the number of metabolites (*m*), the system is under-determined.
183 In order to get a feasible solution space, linear programming (LP), subject to mass
184 balance preservation and flux constraints, was used by introducing an optimization
185 problem. Here, model growth was maximized by maximizing its biomass reaction,
186 which was used as objective function. Specific fluxes for metabolites consumption and
187 secretion were determined following fixation of the respective biomass reaction to its
188 maximal value and then using Flux Variability Analysis (FVA) (Mahadevan and Schilling
189 2003) to calculate possible ranges of these metabolites uptake and secretion. Dynamic

190 modeling was used for the prediction of the profile of consuming metabolites typical
191 to the biomass increase of *P. aurescens* TC1 and atrazine degradation across time. To
192 this end, we simulated the behavior of our metabolic model across time. This was
193 done as described in (Xu et al. 2019) and illustrated in Additional File 5, based on
194 concepts defined in (Harcombe et al. 2014). Briefly, the model works under the
195 following assumptions: (1) A finite start amount of media components is equally
196 available to all members of the population; (2) A maximal amount of uptake a single
197 cell can acquire from the media in a given time point is defined (the lower bound of
198 the exchange reaction value); (3) New substrate concentrations in time t, are
199 determined by the predicted substrate concentration for the previous step
200 augmented with any additional substrates provided or consumed in the current
201 iteration. The maximum uptake of a single organism was set to a ratio of up to 1 unit
202 of each metabolite available in the media to each organism; (4) After each time tick,
203 the biomass amount was updated according to the flux amount of the biomass
204 reaction in the model at this time tick. As biomass production rate serves as a proxy
205 for the size of the population in the simulated environment and substrate
206 uptake/secretion is mainly affected by to population size, the model was used to
207 evaluate the actual substrate uptake/secretion and growth rate given the supplied
208 media across time. Simulations were carried until reaching a state where time cycles
209 did not lead to an increase in biomass. Initial concentration values were set to a fixed
210 amount of 50 units (represented as the initial lower bounds, LB, of the exchange
211 reactions). Simulation parameters and defaults are available in Additional File 6.
212 Starting with one bacterium, the flux balance model was used to predict the uptake

213 of phosphate, sulfate, carbon and nitrogen sources (*i.e.* atrazine and glucose) by *P.*
214 *aurescens* TC1 across time.
215 All model simulations were done on an Intel i7 quad-core server with 32GB of
216 memory, running linux. The development programming language of our simulators
217 was JAVA, and our linear programming software was IBM CPLEX.
218
219 *In vitro* bacterial growth conditions and chemical analysis
220 *P.aurescens* TC1 (ATCC BAA-1386™) was grown on R medium (based on ATCC 2662 R)
221 plates with glucose (0.2%) and atrazine (30 mg/l, Agan Adama -Ashdod, Israel Israel)
222 as sole nitrogen. Stock cultures were maintained in glycerol at -80°C. Cultures were
223 resuscitated on R medium agar plates (1.5% Difco bacto™) and were used as starter
224 colonies for liquid medium growth experiments. The growth of *P.aurescens* TC1 was
225 tested in R media supplemented with different combinations of carbon and nitrogen
226 sources, including Glucose (0.2%), Atrazine (30 mg/l, Agan Adama -Ashdod, Israel),
227 ammonium chloride (37 mg/l), Ethylamine and Isopropylamine (31.1 and 40.8 mg/l,
228 Sigma-Aldrich -Rehovot, Israel) and the amino acids Histidine, Isoleucine and
229 Methionine (36, 92 and 103 mg/l respectively). Concentrations of amino acids,
230 ethylamine and Isopropylamine were calculated to provide the same nitrogen content
231 as the atrazine. In addition to the carbon and nitrogen sources, growth in media
232 supplemented by atrazine and atrazine together with glucose was tested under two
233 phosphate concentrations (K_2HPO_4 in 0.45 and 0.045 g/l). Each substrate was added
234 to sterile R medium and bacteria was grown in triplicate 250ml flasks incubated in
235 30°C with shaking in the dark. One flask contained only R medium and was used as
236 control. A 200 ul sample was taken from each flask every 8 hours for measurement of

237 OD in microplate reader (520nm, Infinite® 200 PRO Tecan, Männedorf Switzerland)
238 and 1 ml was taken to study atrazine degradation rate using HPLC. The HPLC analysis
239 was performed with Agilent 1100 HPLC (Waldbronn Germany) equipped with a DAD
240 detector. Samples were separated on Kinetex C18 column (Phenomenex Torrance, CA)
241 and the mobile phase consisted of 70% methanol flowing at 1 ml/min. Detection and
242 quantitation of atrazine was done at 240 nm with detection limit of 0.1 mg/l. Total
243 duration of each growth experiment was between 152 to 168 hours.

244 Visualizations

245 Venn diagrams were created using Venny (Oliveros 2007). Surface plots were created
246 using the MATLAB 2017b (MathWorks, Inc., Natick, Massachusetts, United States).
247 Pathway maps were created using Escher maps (King et al. 2015).

248 **Results**

249 *P.aurescens* TC1 model construction and validation

250 A genome-scale metabolic model for *P.aurescens* TC1 (*i*RZ960) was reconstructed
251 and curated. Curation procedures were carried iteratively using growth simulations,
252 ensuring the production of all biomass components under the minimal feasible
253 conditions described in Strong et al. (2002). Reconstruction gaps in the initial draft
254 model were manually filled by the addition of *P. aurscens* TC1 reactions retrieved
255 from alternative databases or supported by the literature (Additional File 2). The
256 curated model contains 960 genes, 2322 reactions, out of which 125 are exchange,
257 and 2409 metabolites. Model Reactions involved in atrazine degradation pathway
258 and its further conversion into cellular building blocks are illustrated in Figure 1. As
259 previously reported, *P.aurescens* TC1 degrades atrazine and metabolizes

260 isopropylamine and ethylamine, both can provide sole carbon and nitrogen sources
261 (Strong et al. 2002). Growth simulations confirm that the model captures these
262 reported physiological performances and predictions were directly tested *in vitro*
263 under conditions equivalent to these used for simulations. Experimental growth
264 results verify that atrazine and its degradation products isopropylamine and
265 ethylamine can be used as sole carbon and nitrogen sources for *P. aurscens* TC1
266 (Figure 2A). Supplementing the media with glucose enhanced growth both *in silico*
267 and *in vitro* while supplementing it with ammonia had not shown an effect on
268 bacterial growth. This is in accordance with previous work stating that *P.aurescens*
269 TC1 growth is not inhibited by nitrogen sources such as ammonia (Silva et al.
270 2015).Overall, model simulations corresponded with experimental results and fully
271 repeat previous reports (Figure 2A).

272 Finally, growth simulations under a gradient of nitrogen *vs*. carbon sources further
273 illustrate that atrazine serves as a good nitrogen source and as a poor carbon source
274 (Figure 2B). The growth promoting potential of combinations of atrazine with
275 ammonium (NH_4^+) and glucose as nitrogen and/or carbon sources respectively was
276 tested. The effect of nutrient ratio on growth rate was predicted by optimizing the
277 production of biomass across uptake gradients while constraining the fluxes through
278 exchange reactions for carbon and nitrogen sources. As expected, increasing glucose
279 uptake increased the growth rate (Figure 2B) and the maximal achievable growth
280 rate was much higher with glucose as a carbon source in comparison to atrazine as a
281 sole carbon source. However, atrazine is as equally good nitrogen source as

282 ammonia. This may be endorsed by ammonium as a byproduct of the atrazine
283 degradation process (Figure 1).

284 Effect of media modifications on growth

285 In addition to glucose, several carbon sources were previously reported to enhance
286 growth of several strains of *Arthrobacter* species in atrazine containing media (Guo et
287 al. 2014; Silva et al. 2015). To identify additional media modifications that can
288 potentially increase atrazine degradation, we simulated growth in 123 different media
289 combinations, each supplementing the atrazine containing minimal mineral media
290 with a single exchange metabolite. Several sugars, amino acids and dipeptides were
291 predicted to induce enhanced growth (Additional File 7). This is in accordance with the
292 previous characterization of *P.aurescens* TC1 as a metabolically versatile species
293 (Deutch et al. 2018; Mongodin et al. 2006). Out of a variety of potential nutritional
294 sources, *Paenarthrobacter* species have been shown to utilize different amino acids in
295 different capacities (Dsouza et al. 2015). The effect of amino-acids is media
296 dependent. For example, out of all amino acids tested, Isoleucine has the strongest
297 predicted effect on growth in atrazine containing medium whereas histidine has
298 stronger effect in the medium without atrazine; methionine has the weakest effect in
299 all media (Figure 3). *P.aurescens* TC1 growth in *in vitro* media corresponding to the
300 media used for the *in silica* simulations were generally in agreement with model's
301 predictions supporting the superiority of isoleucine over histidine in atrazine
302 supplemented media but not in the atrazine deficient medium (Figure 3).
303 Supplementing media with methionine showed weaker effect on growth in
304 comparison to the other two amino acids tested, in accordance with its weak effect in

305 the predictions. Prediction and evaluation of the effect of media modifications on
306 atrazine degradation
307 Following the validation of the model predictions for growth capacities, we directly
308 evaluated atrazine degradation performances. To this end, we applied FVA, allowing
309 the identification of the ranges of flux variability that are possible within a given media
310 (Mahadevan and Schilling 2003). Once the biomass flux was maximized, we estimated
311 the rate of atrazine degradation according to the relevant flux. Atrazine degradation
312 over time was simulated in a medium that contains atrazine as a sole carbon and
313 nitrogen source *vs*. modified media sets. Atrazine degradation was estimated
314 according to the amount of atrazine left in the media following each time cycle.
315 Simulations showed that supplementing the media with glucose not only enhances
316 growth (Figure 2) but also induced an enhancement of atrazine consumption.
317 Predictions were confirmed by experimental validation (Figure 4).
318 Finally, the addition of phosphate - a main element in fertilizers, to soils has been
319 reported to have a significant effect on the degradation of herbicides. For instance, its
320 addition was shown to effect soil bacteria's degradation activity including a reported
321 effect on *Arthrobacter* sp. HB-5, a close relative of *P.aurescens* TC1 (Zhang et al. 2014).
322 Phosphate has been previously shown to accelerate atrazine degradation (Kanissery
323 and Sims 2011). We used the genome scale reconstruction to simulate the effect of
324 phosphate on growth and atrazine degradation. In accordance with these reports,
325 simulations showed similar trends, which were confirmed by experimental results,
326 indicating an effect of phosphate concentrations *on P. aurescens* TC1 growth (sup
327 Figure 4) and atrazine degradation (Figure 4).
328 **Discussion**

329 The accumulation and persistence of herbicides and their intermediates in soil and
330 drinking water has long been suggested to be disruptive, imposing a need for effective
331 strategies for their degradation and removal (Zhang et al. 2015). Bioremediation is a
332 widely applied approach for the degradation of herbicides including atrazine (Fan and
333 Song 2014; Megharaj et al. 2011; Nousiainen et al. 2015; Sagarkar et al. 2014; Singh
334 and Singh 2016). Here, we reconstructed a genome scale metabolic model, *i*RZ960, of
335 *P. aurescnes* TC1, a well-known atrazine degrader, in order to use the *in silica*
336 simulations for predicting optimal media to support its growth and atrazine
337 degradation activity. The *in silica* simulations were carried on an array of minimal
338 media using atrazine and its interim degradation products as alternative sole carbon
339 and nitrogen sources supplemented by potential enhancers. The simulations
340 suggested a group of metabolites promoting the increase in biomass yield including
341 sugars, amino acids and dipeptides. We hypothesize that the introduction of such an
342 efficient carbon source leads to an increase in biomass and a subsequent increase in
343 the degradation activity. Simulations were confirmed by *in vitro* experimental
344 validation. This genome scale reconstruction may be used for further experimenting
345 and the gain of new biological knowledge of this metabolically versatile bacteria.
346 While the metabolic modeling approach presented here was demonstrated useful for
347 generating predictions, its limitations should be acknowledged. First, model
348 construction relies on automatic protocols and publically free genomic information.
349 Biomass composition and energy maintenance requirements are hence
350 approximations (Henry et al. 2010; Oh et al. 2007). Second, data used to construct the
351 model is eclectic and annotations were gathered from numerous databases. The lack
352 of data standardization has led to many overlaps and misnomers resulting in draft

353 models containing massive gaps. The lion share of gap filling processes are still done
354 manually due to the differences in data description and cataloging in the different
355 databases. As technology and standardization advance, the process of constructing a
356 metabolic model able to produce testable predictions will be faster and have greater
357 accuracy. Despite relying on genomic data and a growth approximation, resulting
358 predictions are in agreement with experimental observations. We demonstrate that
359 through using metabolic time dependent simulations, an optimal range of nutrient
360 augmentation may be planned. Continuation of the manual curation process, also
361 based on added transcription information, is likely to improve the performances of
362 future versions.
363 Overall, we describe the construction of a mathematical stoichiometric metabolic
364 model of *Paenarthrobacter aurescens* TC1 (*i*RZ960), allowing simulating its
365 degradation activity in contaminated soil. The model successfully predicted both
366 bacterial growth and atrazine degradation in culture. Simulations were used to
367 predict growth and degradation following media modifications such as high/low
368 phosphate content and the addition of variety of amino acids to the standard
369 minimal R medium. Effects of such media were observed experimentally to effect
370 atrazine degradation. *i*RZ960 presented here is shown to be a useful tool for
371 prediction of the metabolic behavior of the bacteria in different media conditions
372 and may be used to further study this versatile organism. Natural degradation of
373 pollutants such as atrazine is of great importance worldwide. A predictive tool such
374 as the presented model is useful for achieving optimal degradation efficiencies.
375 Integration of such models in community models was demonstrated useful for the
376 development of ecologically friendly solutions for pollutant degradation in changing

environments (Xu et al. 2019). The integration of species-specific models together with community approaches is likely to contribute to our understanding of biodegradation processes in natural environments and promote the development of bioaugmentation and biostimulation strategies.

LIST OF ABRAVATIONS

MMM - Minimal Mineral Media; FBA - Flux Balance Analysis; LP -Linear Programming; FVA - Flux Variability Analysis; L/UB – lower/upper bounds.

DECLARATIONS

AVAILABILITY OF DATA AND MATERIALS

All data generated or analyzed during this study are included in this published article and its supplementary information files.

FUNDING

This work was supported by grants from the NSFC-ISF joint program (31461143009), Israel Science Foundation Grant no. 1416/14, and the Science Foundation of Jiangsu Province, China (BK20150670). Atrazine was a gift of Agan Adama (Ashdod, Israel)

AUTHORS' CONTRIBUTIONS

RZ and SO equally contributed to model construction and predicted analysis. TL and X.X., contributed to model curation, testing & development. ZR had designed the experiments and SP and DG carried them. HE, JJ and SF and ZR X.X., R.Z. analyzed the data and designed research. S.O, R.Z., ZR, S.F. and J.J. wrote the manuscript with feedback from all authors.

401 All authors read and approved the final manuscript.

402

403 **COMPETING INTERESTS**

404 None of the authors have any competing interests in the manuscript.

405

406 **REFERENCES**

407

408

409 Abubucker S, Segata N, Goll J, Schubert AM, Izard J, Cantarel BL, Rodriguez-Mueller B,
410 Zucker J, Thiagarajan M, Henrissat B, White O, Kelley ST, Methe B, Schloss PD,
411 Gevers D, Mitreva M, Huttenhower C (2012) Metabolic reconstruction for
412 metagenomic data and its application to the human microbiome. PLoS
413 computational biology 8(6):e1002358 doi:10.1371/journal.pcbi.1002358
414 Adams GO, Fufeyin PT, Okoro SE, Ehinomen I (2015) Bioremediation, biostimulation
415 and bioaugmention: a review. International Journal of Environmental
416 Bioremediation & Biodegradation 3(1):28-39
417 Biswas K, Paul D, Sinha SN (2015) Biological Agents of Bioremediation: A Concise
418 Review. Microbiology 1(3):39-43
419 Burgard AP, Pharkya P, Maranas CD (2003) Optknock: a bilevel programming
420 framework for identifying gene knockout strategies for microbial strain
421 optimization. Biotechnol Bioeng 84(6):647-57 doi:10.1002/bit.10803
422 Chen Q, Wang H, Yang B, He F (2014) The combined effects of atrazine and lead (Pb):
423 relative microbial activities and herbicide dissipation. Ecotoxicol Environ Saf
424 102:93-9 doi:10.1016/j.ecoenv.2014.01.011
425 Contador CA, Rodriguez V, Andrews BA, Asenjo JA (2015) Genome-scale
426 reconstruction of Salinispora tropica CNB-440 metabolism to study strain-
427 specific adaptation. Antonie Van Leeuwenhoek 108(5):1075-90
428 doi:10.1007/s10482-015-0561-9
429 Cordova LT, Long CP, Venkataramanan KP, Antoniewicz MR (2015) Complete genome
430 sequence, metabolic model construction and phenotypic characterization of
431 Geobacillus LC300, an extremely thermophilic, fast growing, xylose-utilizing
432 bacterium. Metab Eng 32:74-81 doi:10.1016/j.ymben.2015.09.009
433 de la Torre A, Metivier A, Chu F, Laurens LM, Beck DA, Pienkos PT, Lidstrom ME,
434 Kalyuzhnaya MG (2015) Genome-scale metabolic reconstructions and
435 theoretical investigation of methane conversion in Methylomicrobium
436 buryatense strain 5G(B1). Microb Cell Fact 14(1):188 doi:10.1186/s12934-015-
437 0377-3

438 Deutch CE, Bui AP, Ho T (2018) Growth of Paenarthrobacter aurescens strain TC1 on
439 atrazine and isopropylamine during osmotic stress. Annals of Microbiology
440 68(9):569-577 doi:10.1007/s13213-018-1364-9
441 Dsouza M, Taylor MW, Turner SJ, Aislabie J (2015) Genomic and phenotypic insights
442 into the ecology of Arthrobacter from Antarctic soils. BMC Genomics 16:36
443 doi:10.1186/s12864-015-1220-2
444 Fan X, Song F (2014) Bioremediation of atrazine: recent advances and promises.
445 Journal of Soils and Sediments 14(10):1727-1737 doi:10.1007/s11368-014-
446 0921-5
447 Fang H, Lian J, Wang H, Cai L, Yu Y (2015) Exploring bacterial community structure and
448 function associated with atrazine biodegradation in repeatedly treated soils. J
449 Hazard Mater 286:457-65 doi:10.1016/j.jhazmat.2015.01.006
450 Fang Y, Scheibe TD, Mahadevan R, Garg S, Long PE, Lovley DR (2011) Direct coupling
451 of a genome-scale microbial in silico model and a groundwater reactive
452 transport model. J Contam Hydrol 122(1-4):96-103
453 doi:10.1016/j.jconhyd.2010.11.007
454 Guo Q, Zhang J, Wan R, Xie S (2014) Impacts of carbon sources on simazine
455 biodegradation by Arthrobacter strain SD3-25 in liquid culture and soil
456 microcosm. International Biodeterioration & Biodegradation 89:1-6
457 Harcombe WR, Riehl WJ, Dukovski I, Granger BR, Betts A, Lang AH, Bonilla G, Kar A,
458 Leiby N, Mehta P, Marx CJ, Segre D (2014) Metabolic resource allocation in
459 individual microbes determines ecosystem interactions and spatial dynamics.
460 Cell reports 7(4):1104-15 doi:10.1016/j.celrep.2014.03.070
461 Henry CS, DeJongh M, Best AA, Frybarger PM, Linsay B, Stevens RL (2010) High-
462 throughput generation, optimization and analysis of genome-scale metabolic
463 models. Nature biotechnology 28(9):977-82 doi:10.1038/nbt.1672
464 Henson MA (2015) Genome-scale modelling of microbial metabolism with temporal
465 and spatial resolution. Biochem Soc Trans 43(6):1164-71
466 doi:10.1042/BST20150146
467 Izallalen M, Mahadevan R, Burgard A, Postier B, Didonato R, Jr., Sun J, Schilling CH,
468 Lovley DR (2008) Geobacter sulfurreducens strain engineered for increased
469 rates of respiration. Metab Eng 10(5):267-75
470 doi:10.1016/j.ymben.2008.06.005
471 Kanehisa M, Goto S (2000) KEGG: kyoto encyclopedia of genes and genomes. Nucleic
472 Acids Res 28 doi:10.1093/nar/28.1.27
473 Kanehisa M, Goto S, Sato Y, Furumichi M, Tanabe M (2012) KEGG for integration and
474 interpretation of large-scale molecular data sets. Nucleic Acids Res
475 40(Database issue):D109-14 doi:10.1093/nar/gkr988
476 Kanehisa M, Goto S, Sato Y, Kawashima M, Furumichi M, Tanabe M (2014) Data,
477 information, knowledge and principle: back to metabolism in KEGG. Nucleic
478 Acids Res 42(Database issue):D199-205 doi:10.1093/nar/gkt1076
479 Kanissery RG, Sims GK (2011) Biostimulation for the Enhanced Degradation of
480 Herbicides in Soil. Applied and Environmental Soil Science 2011:10
481 doi:10.1155/2011/843450
482 Kastner M, Miltner A (2016) Application of compost for effective bioremediation of
483 organic contaminants and pollutants in soil. Appl Microbiol Biotechnol
484 100(8):3433-49 doi:10.1007/s00253-016-7378-y

King ZA, Drager A, Ebrahim A, Sonnenschein N, Lewis NE, Palsson BO (2015) Escher: A Web Application for Building, Sharing, and Embedding Data-Rich Visualizations of Biological Pathways. PLoS computational biology 11(8):e1004321 doi:10.1371/journal.pcbi.1004321

Lee J, Yun H, Feist AM, Palsson BØ, Lee SY (2008) Genome-scale reconstruction and in silico analysis of the Clostridium acetobutylicum ATCC 824 metabolic network. Appl Microbiol Biotechnol 80 doi:10.1007/s00253-008-1654-4

Mahadevan R, Bond DR, Butler JE, Esteve-Nunez A, Coppi MV, Palsson BO, Schilling CH, Lovley DR (2006) Characterization of metabolism in the Fe(III)-reducing organism Geobacter sulfurreducens by constraint-based modeling. Appl Environ Microbiol 72(2):1558-68 doi:10.1128/AEM.72.2.1558-1568.2006

Mahadevan R, Lovley DR (2008) The degree of redundancy in metabolic genes is linked to mode of metabolism. Biophys J 94(4):1216-20 doi:10.1529/biophysj.107.118414

Mahadevan R, Schilling CH (2003) The effects of alternate optimal solutions in constraint-based genome-scale metabolic models. Metabolic engineering 5(4):264-76

Mani D, Kumar C (2013) Biotechnological advances in bioremediation of heavy metals contaminated ecosystems: an overview with special reference to phytoremediation. International Journal of Environmental Science and Technology 11(3):843-872 doi:10.1007/s13762-013-0299-8

Megharaj M, Ramakrishnan B, Venkateswarlu K, Sethunathan N, Naidu R (2011) Bioremediation approaches for organic pollutants: a critical perspective. Environ Int 37(8):1362-75 doi:10.1016/j.envint.2011.06.003

Meyer F, Paarmann D, D'Souza M, Olson R, Glass E, Kubal M, Paczian T, Rodriguez A, Stevens R, Wilke A, Wilkening J, Edwards R (2008) The metagenomics RAST server – a public resource for the automatic phylogenetic and functional analysis of metagenomes. BMC Bioinformatics 9(1):1-8 doi:10.1186/1471-2105-9-386

Monard C, Vandenkoornhuyse P, Le Bot B, Binet F (2011) Relationship between bacterial diversity and function under biotic control: the soil pesticide degraders as a case study. The ISME journal 5(6):1048-56 doi:10.1038/ismej.2010.194

Mongodin EF, Shapir N, Daugherty SC, DeBoy RT, Emerson JB, Shvartzbeyn A, Radune D, Vamathevan J, Riggs F, Grinberg V, Khouri H, Wackett LP, Nelson KE, Sadowsky MJ (2006) Secrets of soil survival revealed by the genome sequence of Arthrobacter aurescens TC1. PLoS Genet 2(12):e214 doi:10.1371/journal.pgen.0020214

Nilsson T, Rova M, Smedja Backlund A (2013) Microbial metabolism of oxochlorates: a bioenergetic perspective. Biochim Biophys Acta 1827(2):189-97 doi:10.1016/j.bbabio.2012.06.010

Nordberg H, Cantor M, Dusheyko S, Hua S, Poliakov A, Shabalov I, Smirnova T, Grigoriev IV, Dubchak I (2014) The genome portal of the Department of Energy Joint Genome Institute: 2014 updates. Nucleic Acids Res 42(Database issue):D26-31 doi:10.1093/nar/gkt1069

Nousiainen AO, Bjorklof K, Sagarkar S, Nielsen JL, Kapley A, Jorgensen KS (2015) Bioremediation strategies for removal of residual atrazine in the boreal

532 groundwater zone. Appl Microbiol Biotechnol 99(23):10249-59
533 doi:10.1007/s00253-015-6828-2
534 Oberhardt MA, Zarecki R, Gronow S, Lang E, Klenk HP, Gophna U, Ruppin E (2015)
535 Harnessing the landscape of microbial culture media to predict new organism-
536 media pairings. Nat Commun 6:8493 doi:10.1038/ncomms9493
537 Oh YK, Palsson BO, Park SM, Schilling CH, Mahadevan R (2007) Genome-scale
538 reconstruction of metabolic network in Bacillus subtilis based on high-
539 throughput phenotyping and gene essentiality data. The Journal of biological
540 chemistry 282(39):28791-9 doi:10.1074/jbc.M703759200
541 Oliveros JC (2007) VENNY. An interactive tool for comparing lists with Venn Diagrams.
542 Orth JD, Thiele I, Palsson BO (2010) What is flux balance analysis? Nat Biotech
543 28(3):245-248
544 doi:http://www.nature.com/nbt/journal/v28/n3/abs/nbt.1614.html#supple
545 mentary-information
546 Perez-Garcia O, Lear G, Singhal N (2016) Metabolic Network Modeling of Microbial
547 Interactions in Natural and Engineered Environmental Systems. Front
548 Microbiol 7:673 doi:10.3389/fmicb.2016.00673
549 Price ND, Papin JA, Schilling CH, Palsson BO (2003) Genome-scale microbial in silico
550 models: the constraints-based approach. Trends Biotechnol 21(4):162-9
551 doi:10.1016/S0167-7799(03)00030-1
552 Reed JL, Vo TD, Schilling CH, Palsson BO (2003) An expanded genome-scale model of
553 Escherichia coli K-12 (iJR904 GSM/GPR). Genome Biol 4(9):R54
554 doi:10.1186/gb-2003-4-9-r54
555 Sagarkar S, Mukherjee S, Nousiainen A, Bjorklof K, Purohit HJ, Jorgensen KS, Kapley A
556 (2013) Monitoring bioremediation of atrazine in soil microcosms using
557 molecular tools. Environ Pollut 172:108-15 doi:10.1016/j.envpol.2012.07.048
558 Sagarkar S, Nousiainen A, Shaligram S, Bjorklof K, Lindstrom K, Jorgensen KS, Kapley A
559 (2014) Soil mesocosm studies on atrazine bioremediation. J Environ Manage
560 139:208-16 doi:10.1016/j.jenvman.2014.02.016
561 Shah J, Dahanukar N (2012) Bioremediation of organometallic compounds by bacterial
562 degradation. Indian J Microbiol 52(2):300-4 doi:10.1007/s12088-011-0223-1
563 Silva VP, Moreira-Santos M, Mateus C, Teixeira T, Ribeiro R, Viegas CA (2015)
564 Evaluation of Arthrobacter aurescens Strain TC1 as Bioaugmentation
565 Bacterium in Soils Contaminated with the Herbicidal Substance
566 Terbuthylazine. PloS one 10(12):e0144978
567 Singh B, Singh K (2016) Microbial degradation of herbicides. Crit Rev Microbiol
568 42(2):245-61 doi:10.3109/1040841X.2014.929564
569 Strong LC, Rosendahl C, Johnson G, Sadowsky MJ, Wackett LP (2002) Arthrobacter
570 aurescens TC1 metabolizes diverse s-triazine ring compounds. Appl Environ
571 Microbiol 68(12):5973-80
572 Thiele I, Palsson BO (2010) A protocol for generating a high-quality genome-scale
573 metabolic reconstruction. Nat Protoc 5(1):93-121 doi:10.1038/nprot.2009.203
574 Thiele I, Vo TD, Price ND, Palsson BO (2005) Expanded metabolic reconstruction of
575 Helicobacter pylori (iIT341 GSM/GPR): an in silico genome-scale
576 characterization of single- and double-deletion mutants. J Bacteriol
577 187(16):5818-30 doi:10.1128/JB.187.16.5818-5830.2005

578 Udikovic-Kolic N, Scott C, Martin-Laurent F (2012) Evolution of atrazine-degrading
579 capabilities in the environment. Appl Microbiol Biotechnol 96(5):1175-89
580 doi:10.1007/s00253-012-4495-0
581 UniProt C (2015) UniProt: a hub for protein information. Nucleic Acids Res
582 43(Database issue):D204-12 doi:10.1093/nar/gku989
583 Varma A, Palsson BO (1994) Stoichiometric flux balance models quantitatively predict
584 growth and metabolic by-product secretion in wild-type Escherichia coli
585 W3110. Applied and environmental microbiology 60(10):3724-3731
586 Wang Q, Xie S (2012) Isolation and characterization of a high-efficiency soil atrazine-
587 degrading Arthrobacter sp. strain. International Biodeterioration &
588 Biodegradation 71:61-66 doi:10.1016/j.ibiod.2012.04.005
589 Xie S, Wan R, Wang Z, Wang Q (2013) Atrazine biodegradation by Arthrobacter strain
590 DAT1: effect of glucose supplementation and change of the soil microbial
591 community. Environ Sci Pollut Res Int 20(6):4078-84 doi:10.1007/s11356-012-
592 1356-4
593 Xu C, Liu L, Zhang Z, Jin D, Qiu J, Chen M (2013) Genome-scale metabolic model in
594 guiding metabolic engineering of microbial improvement. Appl Microbiol
595 Biotechnol 97(2):519-39 doi:10.1007/s00253-012-4543-9
596 Xu X, Zarecki R, Medina S, Ofaim S, Liu X, Chen C, Hu S, Brom D, Gat D, Porob S,
597 Eizenberg H, Ronen Z, Jiang J, Freilich S (2019) Modeling microbial
598 communities from atrazine contaminated soils promotes the development of
599 biostimulation solutions. The ISME journal 13(2):494-508 doi:10.1038/s41396-
600 018-0288-5
601 Zhang C, Li Y, Wang C, Niu L, Cai W (2015) Occurrence of endocrine disrupting
602 compounds in aqueous environment and their bacterial degradation: A review.
603 Critical Reviews in Environmental Science and Technology 46(1):1-59
604 doi:10.1080/10643389.2015.1061881
605 Zhang Q, Zhu L, Su J, Wang J, Xie H, Wang J, Wang F (2014) Impacts of nitrogen and
606 phosphorus on atrazine-contaminated soil remediation and detoxification by
607 Arthrobacter sp. strain HB-5. Environmental earth sciences 71(3):1465-1471
608 Zhang Y, Cao B, Jiang Z, Dong X, Hu M, Wang Z (2012) Metabolic ability and individual
609 characteristics of an atrazine-degrading consortium DNC5. J Hazard Mater 237-
610 238:376-81 doi:10.1016/j.jhazmat.2012.08.047
611 Zomorrodi AR, Segre D (2016) Synthetic Ecology of Microbes: Mathematical Models
612 and Applications. J Mol Biol 428(5 Pt B):837-61 doi:10.1016/j.jmb.2015.10.019
613 Zou W, Liu L, Zhang J, Yang H, Zhou M, Hua Q, Chen J (2012) Reconstruction and
614 analysis of a genome-scale metabolic model of the vitamin C producing
615 industrial strain Ketogulonicigenium vulgare WSH-001. J Biotechnol 161(1):42-
616 8 doi:10.1016/j.jbiotec.2012.05.015

617

618 **FIGURE LEGENDS**

619

620 Figure 1. Atrazine metabolism as implemented in the cytoplasm compartment of *P.*
621 *aurescens* TC1 genome scale metabolic model reconstruction (*i*RZ960). External
622 metabolite are notated with an e0;
623
624 Figure 2. Growth performances of *P.aurescens* TC1 in dependence on the availability
625 of different carbon and nitrogen sources. (A) Predicted and observed *A.aurescens* TC1
626 growth in mineral minimal media supplemented with Atrazine or its degradation
627 intermediates. ATZ-Atrazine, NH4, GLU-Glucose, ETH - Ethylamine, ISO –
628 Isopropylamine, CTRL - control. Values are normalized by dividing in maximal value.
629 (B) Surface plot rendering *P.aurescens* TC1 growth (biomass) in dependence on
630 atrazine, glucose and NH4 availability. Color scale is indicative of biomass (Z-axis).
631
632 Figure 3. Predicted and observed growth performances of *P. aurescens* TC1 growth in
633 mineral minimal media with glucose complemented by different amino acids and
634 atrazine. ATZ-Atrazine, HIS- Histdine, ILE-Isoluecine and MET- Metionine. Observed
635 values represents mean in triplicates; bars represent SD.
636
637 Figure 4. Predicted and observed atrazine degradation in modified media. High and
638 low phosphate concentrations: 50 and 5 mmol/gdw h for predicted and 0.081 and
639 0.081 g/l for observed, respectively. ATZ- atrazine, GLU- glucose. Observed values
640 represents mean in triplicates; bars represent SD.
641
642
643 **ADDITIONAL FILES**

644

645 Additional File 1. Supplementary Figure 1 (tiff). Venn diagram of *P.aurescens* TC1
646 annotations collected from four established databases.

647 Additional File 2. Table (xlsx). Reactions added to the model in the process of manual
648 curation and gap filling.

649 Additional File 3. Table (xlsx). Alternative carbon and nitrogen sources added to the
650 minimal mineral media used for *P.aurescens* TC1 growth.

651 Additional File 4. Metabolic model (sbml). *P.* aurescens TC1 metabolic model (iRZ960)
652 file.

653 Additional File 5. Supplementary Figure 2 (tiff). A schematic diagram describing a time
654 dependent simulation of nutrient dependent bacterial growth.

655 Additional File 6. Table (xlsx). Default values for exchange reactions as used for all
656 simulations.

657 Additional File 7. Table (xlsx). FVA analysis for different metabolites added to an
658 atrazine containing mineral media.

659 Additional File 8. Supplementary Figure 3 (tiff). Predicted and observed *P.aurescens*
660 TC1 growth in media supplemented with high and low phosphate concentrations (50
661 and 5 mmol/gdw h for predicted and 0.081 and 0.081 g/l for observed respectively).
662 Simulations and experiments were carried in MMM supplemented with atrazine and
663 glucose in ATZ-Atrazine, GLU-Glucose. Observed values represents mean in triplicates;
664 bars represent SD.

665

666

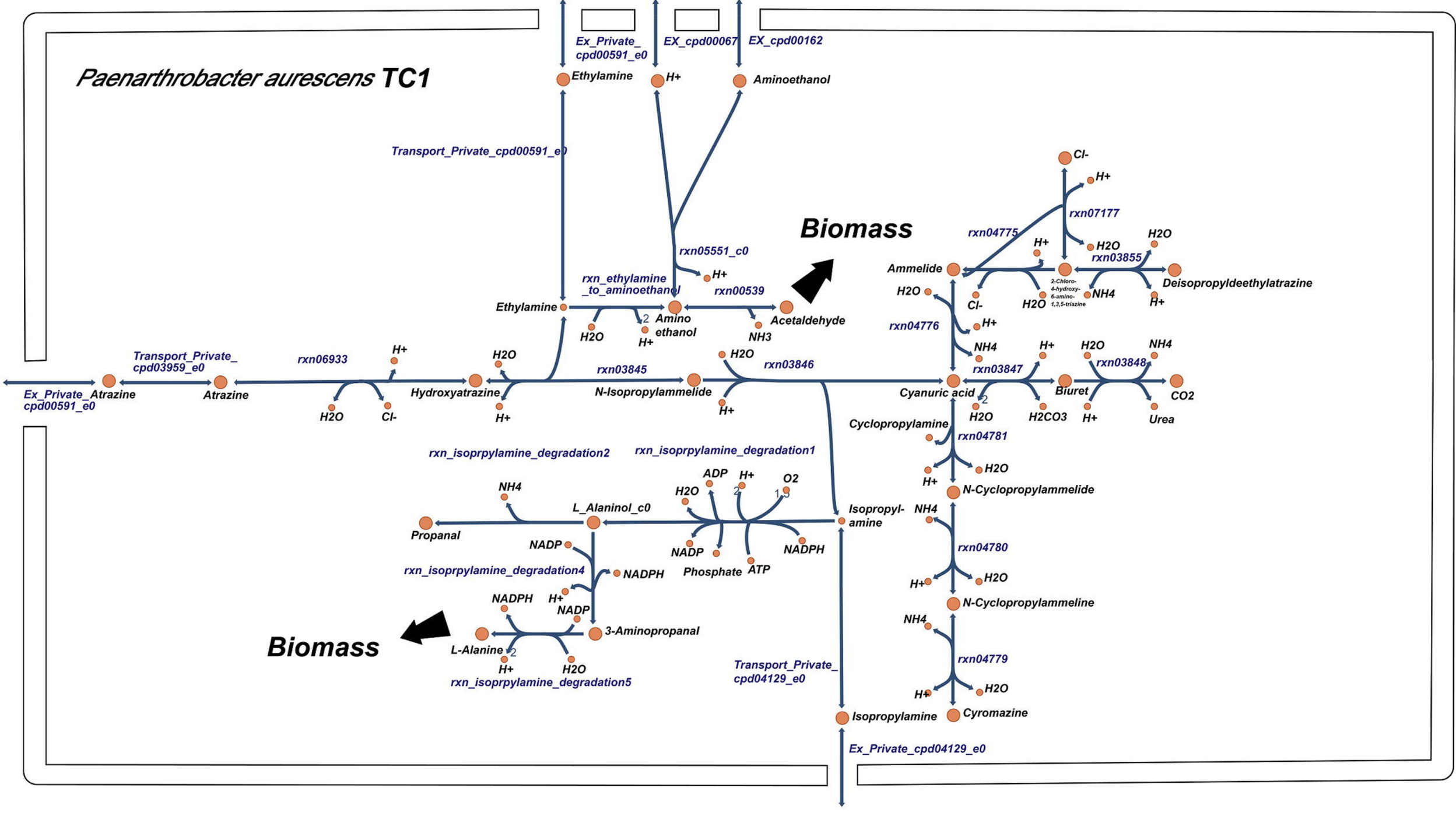
Paenarthrobacter aurescens TC1
Ex_Private_ cpd00591_e0
EX_cpd00067
EX_cpd00162
Ethylamine
H+
Aminoethanol
Transport_Private_cpd00591_e0
rxn05551_c0
H+
rxn_ethylamine _to_aminoethanol
rxn00539
Ethylamine
2
Amino ethanol
Acetaldehyde
H2O
H+
NH3
Biomass
Cl-
H+
rxn07177
rxn04775
H+
H2O
H2O
rxn03855
Ammelide
2-Chloro-4-hydroxy-6-amino-1,3,5-triazine
Deisopropyldeethylatrazine
H2O
Cl-
H2O
NH4
H+
rxn04776
H+
NH4
Transport_Private_ cpd03959_e0
rxn06933
H+
H2O
H2O
rxn03845
H2O
rxn03846
H+
rxn03847
H+
H2O
NH4
rxn03848
Ex_Private_Atrazine cpd00591_e0
Atrazine
Hydroxyatrazine
N-Isopropylammelide
Cyanuric acid
2
Biuret
CO2
H2O
Cl-
H+
H+
H2O
H2CO3
H+
Urea
Cyclopropylamine
rxn04781
rxn_isoprpylamine_degradation2
rxn_isoprpylamine_degradation1
ADP
H+
O2
H2O
2
1,3
H+
H2O
N-Cyclopropylammelide
NH4
L_Alaninol_c0
Isopropyl- amine
NH4
Propanal
NADP
NADP
NADPH
rxn04780
rxn_isoprpylamine_degradation4
NADPH
Phosphate
ATP
H+
H2O
NADPH
H+
NADP
N-Cyclopropylammeline
NH4
3-Aminopropanal
Biomass
L-Alanine
2
H+
H2O
rxn_isoprpylamine_degradation5
Transport_Private_ cpd04129_e0
rxn04779
H+
H2O
Isopropylamine
Cyromazine
Ex_Private_cpd04129_e0

A

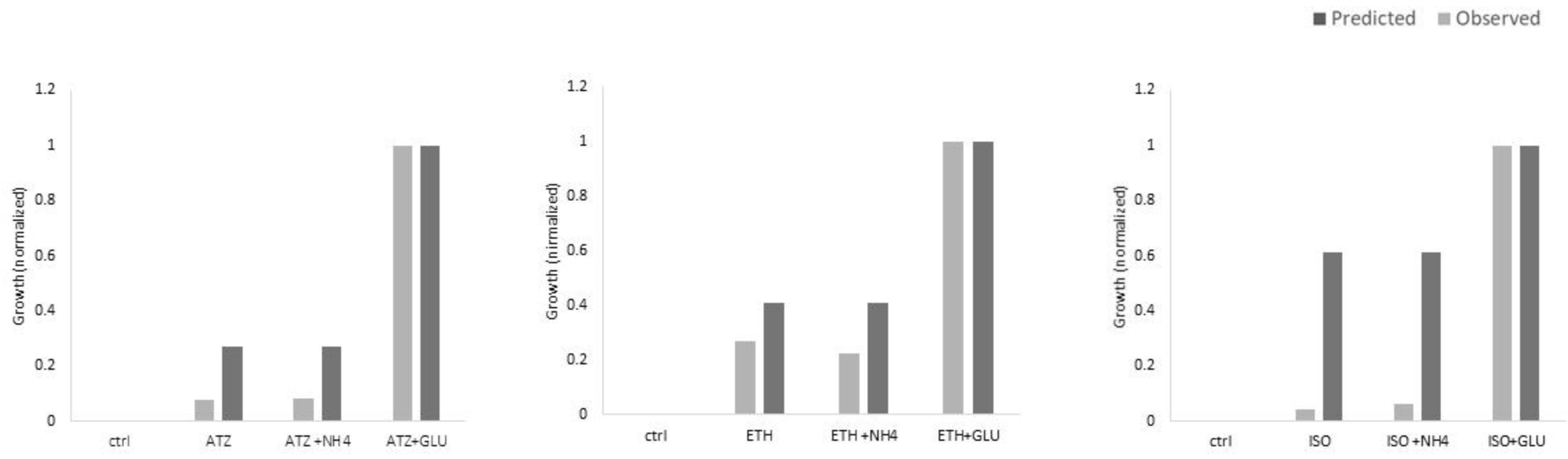
Predicted
Observed
Growth (normalized)
1.2
1
0.8
0.6
0.4
0.2
0
ctrl
ATZ
ATZ +NH4
ATZ+GLU
Growth (nirmalized)
ctrl
ETH
ETH +NH4
ETH+GLU
Growth (normalized)
ctrl
ISO
ISO +NH4
ISO+GLU

B

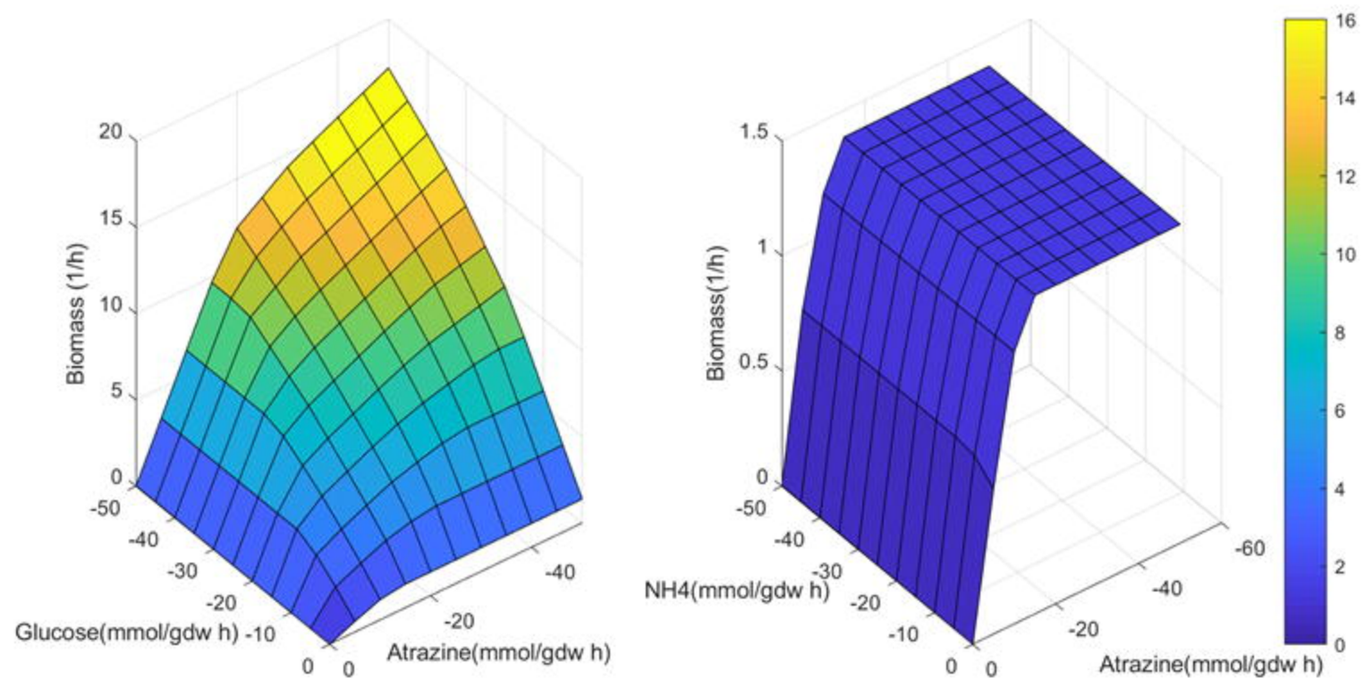
Biomass (1/h)
20
15
10
5
0
-50
-40
-30
-20
-10
0
Glucose(mmol/gdw h)
0
-20
-40
Atrazine(mmol/gdw h)
Biomass(1/h)
1.5
1
0.5
0
-50
-40
-30
-20
-10
0
NH4(mmol/gdw h)
0
-20
-40
-60
Atrazine(mmol/gdw h)
16
14
12
10
8
6
4
2
0

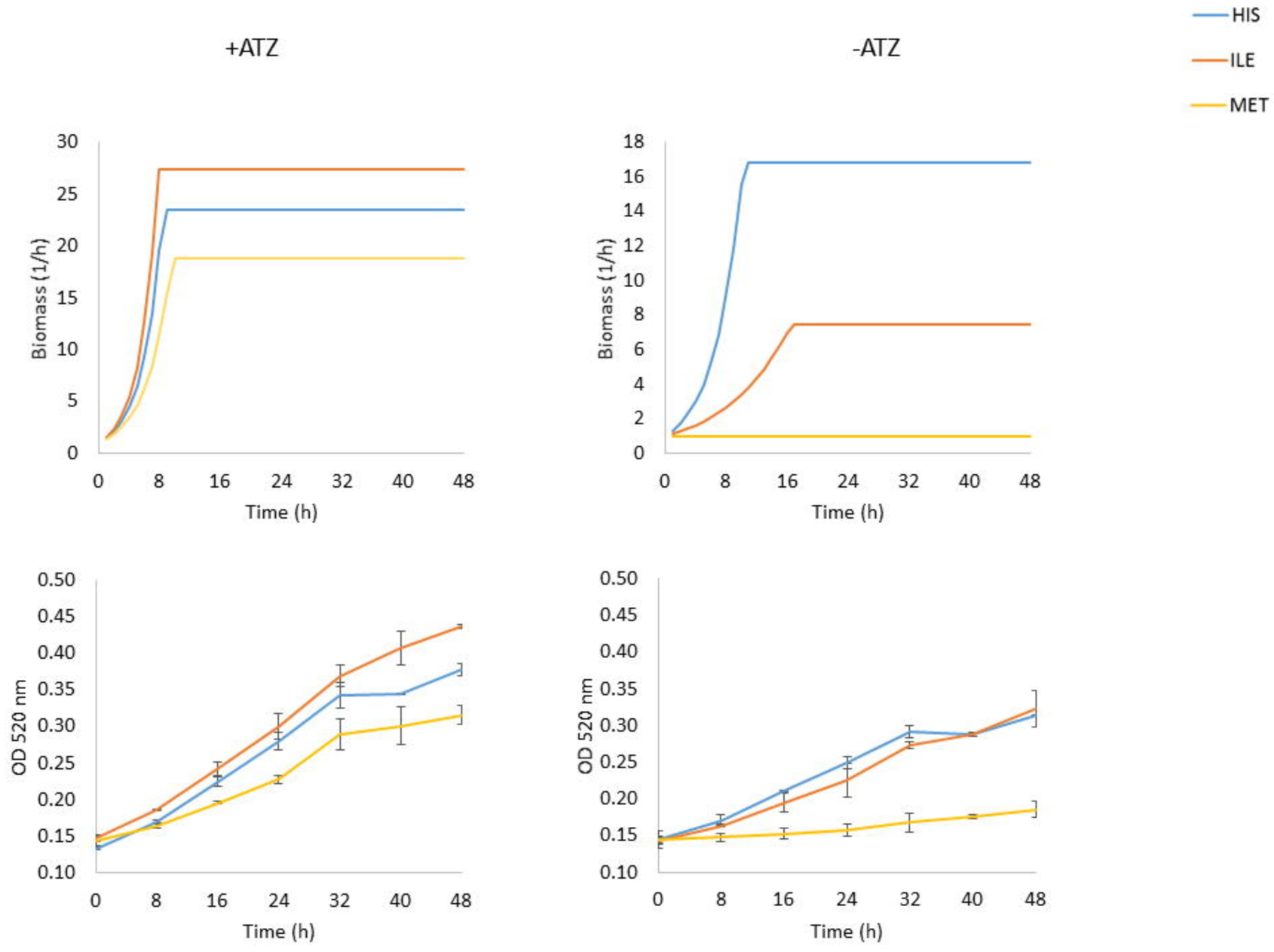
+ATZ
-ATZ
HIS
ILE
MET
Biomass (1/h)
Time (h)
OD 520 nm
0
8
16
24
32
40
48
0
5
10
15
20
25
30
0
2
4
6
8
10
12
14
16
18
0.10
0.15
0.20
0.25
0.30
0.35
0.40
0.45
0.50

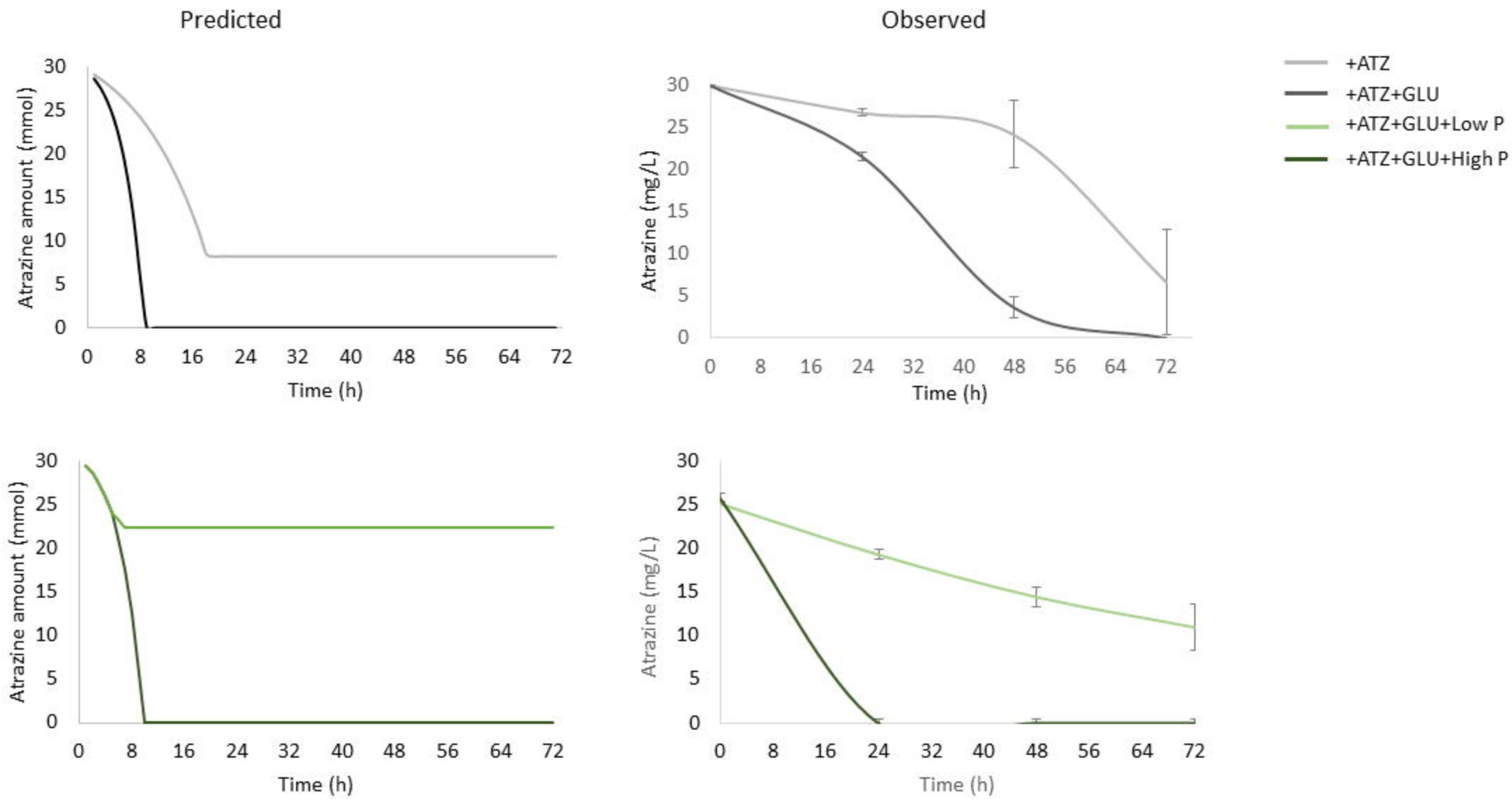
Predicted
Observed
Atrazine amount (mmol)
Atrazine (mg/L)
Time (h)
0
8
16
24
32
40
48
56
64
72
0
5
10
15
20
25
30
+ATZ
+ATZ+GLU
+ATZ+GLU+Low P
+ATZ+GLU+High P